npj | flexible electronics

Article

Published in partnership with Nanjing Tech University

https://doi.org/10.1038/s41528-026-00542-8

Breathable nanomesh electrodes with improved water resistance and stretchability for skin impedance monitoring

Maho Mimuro[1], Yusuke Ebihara[1], Xiaoping Liang[1], Daishi Inoue[2], Daisuke Hashizume[2], Sunghoon Lee[1,2,3], Tomoyuki Yokota[1,4], Kento Yamagishi[1] & Takao Someya[1,2,3] ✉

Skin impedance reflects both the barrier function and psychophysiological state of the human body, but long-term monitoring remains challenging due to the lack of electrodes that simultaneously offer water resistance, stretchability, and breathability. In this study, we developed poly(vinyl alcohol)/waterborne polyurethane (PVA/WBPU) blend nanomesh electrodes with controlled polymer composition to address these requirements. Electrospinning produced nanofibers with an island–sea morphology, where partial dissolution of PVA enabled temporary skin adhesion while residual WBPU maintained structural integrity. The optimized PVA/WBPU = 5/5 electrodes showed minimal resistance increase (1.02-fold) after 24 h of continuous water flow and retained conductivity under 80% strain and after 1000 stretch cycles. When applied to the palm, they maintained stable resistance ($< 50\ \Omega$) for at least 4 h, whereas PVA-only electrodes frequently exhibited resistance increases above 1 kΩ or electrical disconnection. These results indicate that controlling the PVA/WBPU blending ratio ensures mechanical and electrical stability while preserving breathability, establishing a materials design strategy for long-term, skin-conformable, and breathable bioelectronic interfaces.

Skin impedance has been studied as an indicator for quantitative evaluation of the barrier function of the stratum corneum[1–3] and for detection of psychological stress levels[4,5], and plays an important role in medical and physiological monitoring. Because skin impedance is influenced by transepidermal water loss and perspiration, continuous measurement over a period ranging from several hours to days is expected to enable early detection and monitoring of skin diseases such as atopic dermatitis[6], as well as stress assessment. Sweating on the palm and sole is induced by psychological stress rather than thermoregulatory mechanisms, and quantifying this response through skin impedance is useful for evaluating autonomic dysfunctions and psychiatric disorders[7,8].

Water continuously evaporates from the skin, and perspiration can further increase water release. In addition, skin is soft, with a Young's modulus of 0.4–0.85 MPa, and undergoes constant deformation[9]. Electrodes intended for stable long-term skin impedance measurement therefore require the following properties: (1) water resistance against sweat and moisture, (2) stretchability to follow natural skin deformation, and (3) breathability to allow physiological evaporation. Breathability is critical because it directly affects measurement accuracy[10]. Previous approaches have developed thin-film electrodes using conductive pastes or elastomers with durability against water and strain[11,12], as well as paste-like electrodes composed of ionic or polymeric materials[13,14]. These designs have enabled short-term (<1 h) skin impedance measurements.

For longer-term measurement, strategies to improve breathability include reducing electrode area or employing fiber-based structures. As an example of the former approach, serpentine-patterned graphene–gold thin-film electrodes have been demonstrated[15], achieving continuous measurement of palmar skin conductance for up to 16 h. This strategy highlights the potential of miniaturized electrode designs for extended monitoring, although the reduced contact area is known to increase contact impedance, which can affect measurement accuracy[16,17]. Nanomesh electrodes represent the latter approach, and their porous architecture has enabled continuous skin resistance measurement for up to 12 h[10,18]. However, nanomesh electrodes fabricated from poly(vinyl alcohol) (PVA) require partial dissolution

[1]Department of Electrical Engineering and Information Systems, The University of Tokyo, Bunkyo-ku, Tokyo, Japan. [2]RIKEN Center for Emergent Matter Science (CEMS), Wako, Saitama, Japan. [3]Thin-Film Device Laboratory, RIKEN, Wako, Saitama, Japan. [4]Institute of Engineering Innovation, Graduate School of Engineering, The University of Tokyo, Bunkyo-ku, Tokyo, Japan. ✉e-mail: someya@ee.t.u-tokyo.ac.jp

of PVA for adhesion to skin. This adhesion deteriorates under exposure to sweat or water, and the gold nanomesh remaining after dissolution exhibits limited stretchability and mechanical robustness, often fracturing under small strains. Consequently, long-term stable impedance measurement on the palm, where perspiration and mechanical stress are significant, has not been demonstrated.

In this study, the blending ratio of poly(vinyl alcohol) (PVA) and waterborne polyurethane (WBPU) was systematically optimized to develop nanomesh electrodes that retain breathability while exhibiting improved water resistance and stretchability. The incorporation of WBPU into the PVA nanofiber matrix reinforces the mesh structure after partial dissolution of PVA, which acts as a transient adhesive for skin attachment, thereby balancing adhesion and durability—two properties that have been difficult to achieve simultaneously in conventional PVA-based nanomesh electrodes. The optimized PVA/WBPU = 5/5 composition maintained stable electrical resistance and mechanical integrity for at least 4 h even on the palm, where perspiration and motion impose severe stress, without compromising breathability. These findings demonstrate that controlling the polymer composition in nanofiber networks is an effective strategy for achieving mechanically robust and electrically stable breathable nanomesh electrodes, providing a foundation for long-term, noninvasive monitoring on dynamic and high-sweat skin regions.

Results and discussion

Overview of the study

In this study, we developed gas-permeable, water-resistant, and strain-tolerant nanomesh electrodes composed of blended polyvinyl alcohol (PVA) and waterborne polyurethane (WBPU) for long-term monitoring of skin impedance and resistance. As illustrated in Fig. 1a and b, the electrode consists of electrospun PVA/WBPU nanofibers coated with a thin gold layer. When water is sprayed on the electrode attached to skin, part of the PVA dissolves, acting as an adhesive that anchors the electrode, while the WBPU remains as residual tubular fibers that preserve the mesh architecture. This unique structural transformation enables conformal contact with the skin surface without the need for external adhesives.

The fiber structure, with diameters in the range of 300–900 nm (Fig. S1a), ensures excellent breathability, while the total thickness of only a few micrometers allows intimate conformity to fine epidermal microstructures (Fig. S1b). The electrodes adhere spontaneously upon slight hydration and maintain robust attachment even under exposure to water (Fig. 1c), while retaining mechanical flexibility and stretchability during skin deformation (Fig. 1d). These combined properties allow stable impedance measurement on perspiration-prone areas such as the palm, where conventional PVA-based nanomesh electrodes readily fail. Consequently, the PVA/WBPU blend nanomesh electrodes achieve reliable long-term skin impedance monitoring, expanding their applicability to continuous measurements during daily activities, including stress evaluation, exercise monitoring, and sleep studies.

Fabrication of PVA/WBPU blend nanofibers using electrospinning

Electrospun nanofibers were fabricated from different polymer solutions. The PVA-only nanofibers were prepared from a 10 wt% aqueous PVA solution, whereas the blend nanofibers were obtained by mixing a 15 wt% PVA solution with a 30 wt% WBPU dispersion at defined ratios. The mixing ratio refers to the weight ratio of solid polymer components (PVA:WBPU). As shown in Fig. S2, nanofibers with PVA/WBPU ratios of 9/1, 7/3, and 5/5 exhibited homogeneous fiber morphologies with diameters of 300–900 nm, comparable to those of PVA-only fibers. In contrast, nanofibers with a ratio of 3/7 exhibited non-uniform diameters, and those with a ratio of 1/9 contained numerous beads with diameters of 1–3 μm as well as ultrathin fibers (<100 nm) (see Fig. S2). These results indicate that blend solutions with low viscosity, particularly at ratios of 3/7 and 1/9, are unsuitable for fabricating mechanically stable electrodes. The viscosity of the polymer solution is a critical factor in electrospinning, as it governs the balance between the applied electric field and the surface tension of the solution, thereby determining the fiber morphology[19,20]. The viscosity data of the polymer blend solutions (Fig. S3) confirm that the reduced viscosity at high WBPU content accounts for the poor fiber morphology. Based on these findings, subsequent experiments focused on PVA-only, PVA/WBPU = 7/3, and PVA/WBPU = 5/5 compositions.

Representative SEM images of nanofiber surfaces for PVA-only, 7/3, and 5/5 are shown in Fig. 2a–c. These images are identical to those presented in Fig. S1 for direct comparison of fiber morphologies across all blend ratios. Cross-sectional SEM images (Fig. 2d–f) revealed that while PVA-only fibers exhibited a homogeneous internal structure (Fig. 2f), the 7/3 and 5/5 blends

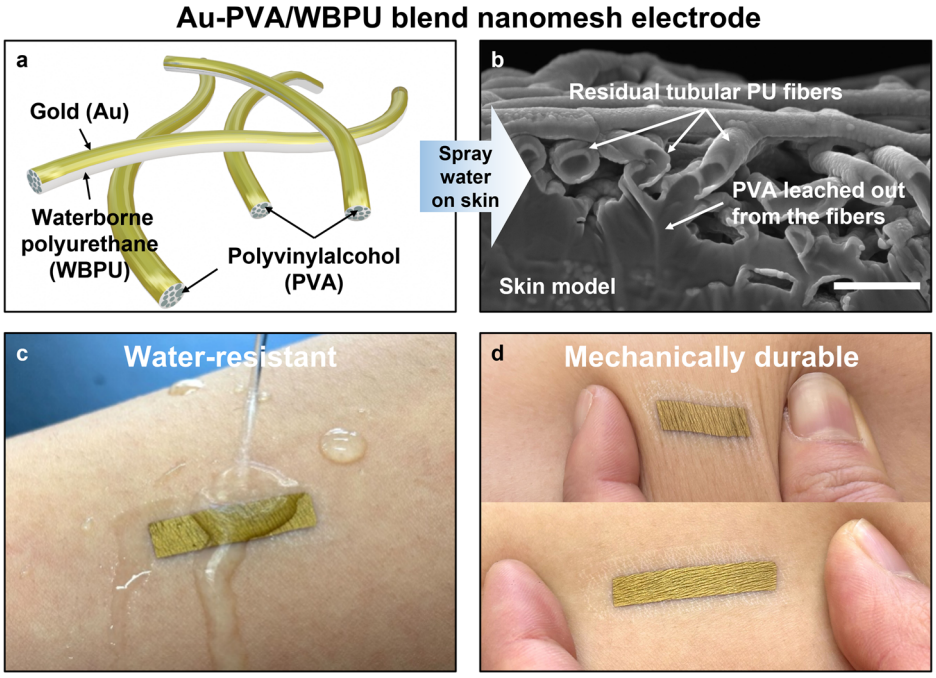

Fig. 1 | Au–PVA/WBPU blend nanomesh electrode and its application on skin. a Schematic illustration of the nanomesh electrode composed of polyvinyl alcohol (PVA) and waterborne polyurethane (WBPU) nanofibers coated with a thin gold (Au) layer. The WBPU component imparts water resistance and stretchability, while PVA enables temporary water-induced adhesion to the skin. Scale bar = 2 μm. **b** Cross-sectional scanning electron microscopy (SEM) image of the electrode conformally attached to a skin model after spraying water, showing intimate integration of the porous nanomesh structure with the skin model surface. **c** Photograph demonstrating that the electrode remains firmly attached and intact even when water is poured onto the skin, indicating high water resistance and structural robustness. **d** Photographs showing that the electrode maintains conformal adhesion and mechanical integrity during repeated skin stretching and relaxation, confirming excellent mechanical durability.

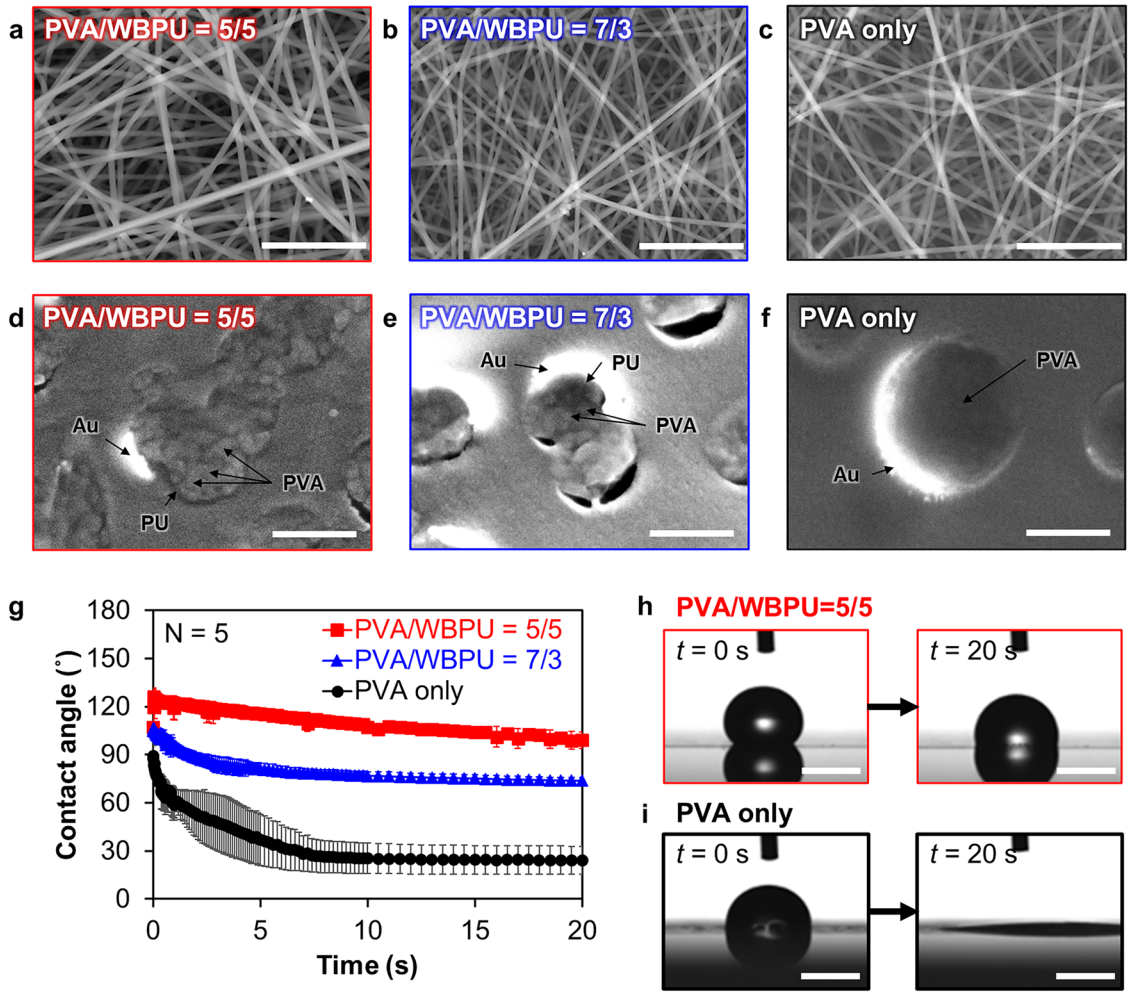

Fig. 2 | Structure and surface hydrophobicity of PVA/WBPU blend nanomesh electrodes. Surface SEM images of electrospun nanofibers composed of PVA/WBPU blends with ratios of **a** 5/5, **b** 7/3, and **c** PVA only. The blend nanofibers maintained uniform diameters in the submicrometer range, whereas PVA-only fibers showed smoother but less stable morphology. Scale bars = 10 μm. Cross-sectional SEM images of Au-coated nanofibers for PVA/WBPU = 5/5 (**d**), PVA/WBPU = 7/3 (**e**), and PVA-only (**f**) samples. Arrows indicate the Au nanolayer, PVA-rich domains, and the PU matrix, as labeled. The blend fibers exhibit a phase-separated morphology in which PVA-rich domains are embedded within a continuous PU matrix, whereas the PVA-only fibers show a homogeneous internal structure. Scale bars = 500 nm. **g** Contact angle measurements of nanomesh electrodes with different PVA/WBPU ratios. Electrodes containing WBPU exhibited significantly higher water contact angles compared with PVA-only electrodes, indicating enhanced surface hydrophobicity and improved water resistance. Representative photographs of water droplet contact angles on **h** PVA/WBPU = 5/5 and **i** PVA-only nanomesh electrodes immediately after water deposition (t = 0 s) and after 20 s. Droplets on the WBPU-containing nanomesh retained their spherical shape, while those on the PVA-only nanomesh rapidly spread due to water absorption. Scale bars = 0.5 mm.

(Fig. 2e, d) showed heterogeneous morphologies with multiple island-like domains embedded within a continuous matrix. The domains were larger in the 7/3 fibers compared with the 5/5 fibers. These observations suggest a phase-separated configuration, where PVA forms dispersed domains and WBPU constitutes the continuous matrix, resembling an island–sea morphology. These observations suggest a phase-separated configuration, where PVA forms dispersed domains and WBPU constitutes the continuous matrix, resembling an island–sea morphology. While cross-sectional SEM images confirm the presence of phase separation, they do not allow unambiguous determination of whether the PVA-rich domains are fiber-like or particle-like in three-dimensional geometry. However, the consistent observation of phase-separated structures across all fiber cross-sections, together with the formation of hollow PU-supported structures after PVA dissolution, suggests that the PVA domains are likely elongated along the fiber direction.

To evaluate surface hydrophobicity, water contact angle measurements were conducted (Fig. 2g–i). The PVA-only nanomesh (Fig. 2i) rapidly absorbed water, resulting in complete disintegration within 5–10 s. In contrast, blend nanomesh electrodes incorporating WBPU showed enhanced hydrophobicity, with contact angles increasing in proportion to WBPU content. At 20 s, the contact angles were 74 ± 1° for 7/3 and 96 ± 2° for 5/5 (Fig. 2h), confirming their enhanced hydrophobic properties. To quantitatively evaluate wettability, water contact angle measurement was employed as a standard method for assessing surface free energy[21] These results indicate that WBPU is enriched at the fiber surface, consistent with the island (PVA)–sea (PU) configuration suggested by cross-sectional SEM analysis.

Stability of nanomesh electrodes against water exposure

To evaluate the water resistance of the prepared nanomesh electrodes, electrical resistance was measured under continuous water (22 °C) flow using the setup shown in Fig. 3a (see also Movie S1). The results are summarized in Fig. 3b. Water flow was initiated at 60 s (x = 1 on the time axis). PVA-only electrodes (PVA/WBPU = 10/0) lost conductivity after only 36 s. In contrast, the PVA/WBPU = 7/3 electrode showed a modest 1.1-fold increase in resistance immediately after the onset of water flow but remained

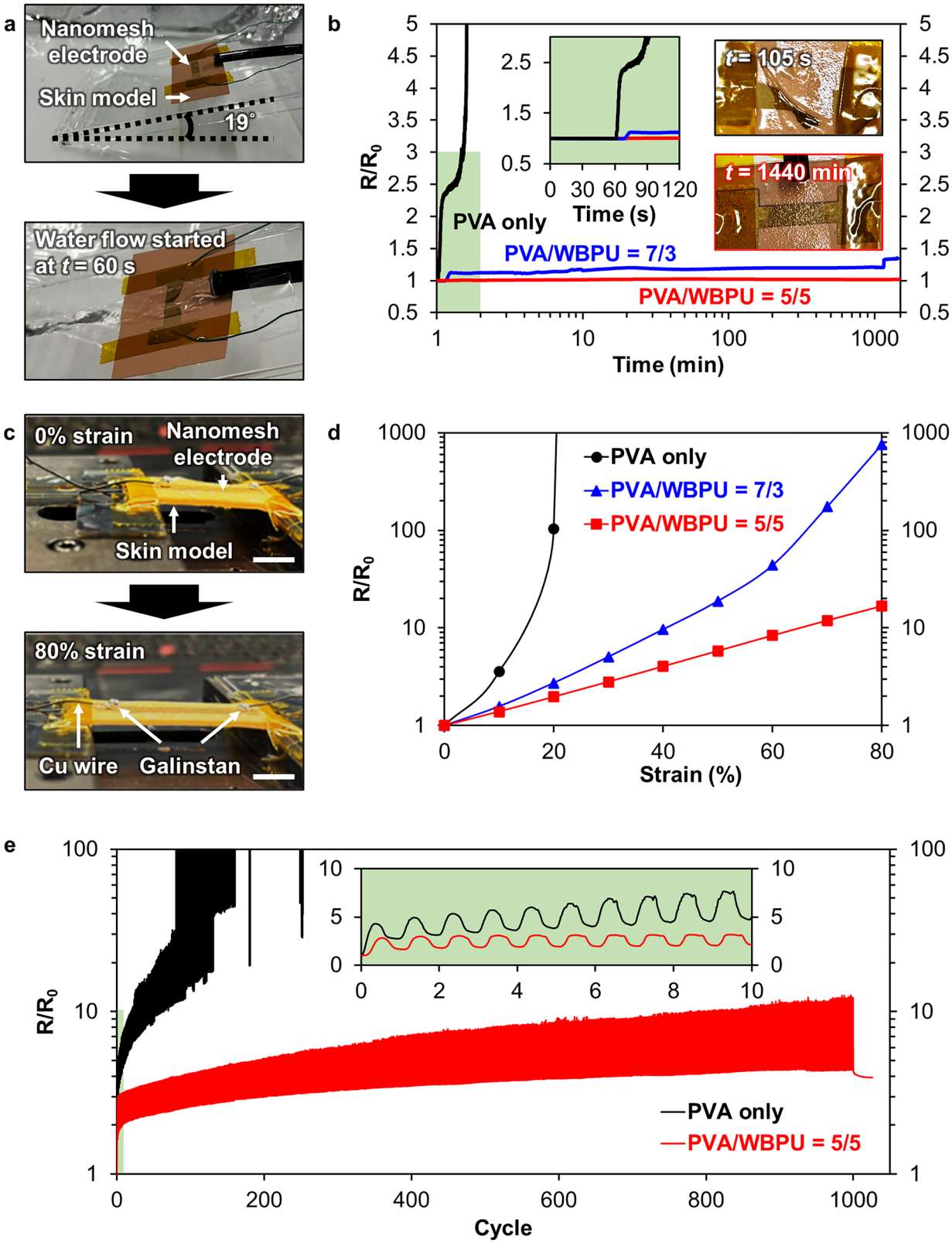

Fig. 3 | Electromechanical stability of PVA/WBPU blend nanomesh electrodes. **a** Photographs of the experimental setup for the water-stability test, in which the nanomesh electrode was laminated on a skin model and tilted at 19°. Water flow was initiated after 60 s. **b** Relative resistance changes of nanomesh electrodes composed of PVA/WBPU = 5/5 and 7/3 blends during continuous water flow. Electrodes containing a higher fraction of WBPU exhibited markedly improved water stability, maintaining electrical conductivity for over 1440 min, while PVA-only electrodes lost conductivity within 105 s. Insets show optical images of the electrodes at the respective times. **c** Photographs of the stretchability test, where nanomesh electrodes connected with Cu wires and Galinstan liquid metal contacts were stretched on a skin model. Scale bar = 1 cm. **d** Relative resistance as a function of applied strain for electrodes with different blend ratios. The PVA/WBPU = 5/5 electrode maintained low resistance change up to 80% strain, demonstrating superior mechanical robustness. **e** Cyclic electromechanical stability under 20% repeated strain. The PVA/WBPU = 5/5 electrode showed stable resistance with minimal drift over 1000 cycles, whereas electrodes with lower WBPU content exhibited progressive resistance increases and eventual failure.

stable thereafter. The PVA/WBPU = 5/5 electrode exhibited the highest durability, with only a 1.02-fold increase in resistance even after 24 h of continuous water flow. Room-temperature water was selected as a reproducible baseline condition, as perspiration secreted from the skin is rapidly exposed to ambient air and typically equilibrates close to room temperature, particularly on exposed regions such as the palm. The practical relevance of this condition is further discussed in the context of on-skin measurements presented below.

Optical microscopy observations further clarify the origin of this enhanced water stability. As shown in Fig. S4, after water exposure the PVA-only nanomesh loses its fibrous morphology, leaving a cracked and discontinuous Au film. In contrast, the PVA/WBPU = 5/5 blend nanomesh retains a fibrous structure after water exposure, indicating that the residual PU fibers remain and act as a mechanical scaffold supporting the Au nanolayer. This structural preservation explains the sustained electrical conductivity of the PVA/WBPU = 5/5 electrodes under prolonged water exposure.

In addition, qualitative adhesion stability was evaluated for the PVA/WBPU = 5/5 electrodes using a skin model before and after 24 h water immersion. A Kapton tape (adhesion strength ~1.25 N cm^{-1}) was used as a reference peeling layer. While the nanomesh was largely removed immediately after attachment, complete retention was observed after 24 h immersion, indicating enhanced interfacial conformity and adhesion after PVA dissolution (Fig. S5). This enhanced adhesion is likely attributed to the formation of hollow PU fiber structures after PVA removal, which conform more intimately to the skin model surface and thereby increase effective interfacial contact.

Taken together, these results demonstrate that blending PVA with WBPU significantly enhances both the electrical and interfacial stability of nanomesh electrodes under wet conditions. While PVA-only electrodes rapidly lose conductivity due to dissolution and structural collapse, the PVA/WBPU = 5/5 electrodes maintain electrical continuity even under continuous water flow for 24 h and simultaneously exhibit improved adhesion after prolonged water immersion. The dissolution of PVA leads to the formation of a PU-supported Au nanomesh that conforms more intimately to the skin surface, thereby stabilizing both electrical performance and effective skin adhesion. These combined properties make the PVA/WBPU = 5/5 composition particularly suitable for long-term, continuous skin impedance monitoring in sweat-prone and humid environments.

Electromechanical properties of nanomesh electrodes

The stretchability of the nanomesh electrodes was evaluated using the setup shown in Fig. 3c. Figure 3d presents the relationship between strain and resistance change for each electrode. The PVA-only electrode (PVA/WBPU = 10/0) ruptured and lost electrical conductivity at 20–30% strain. In contrast, the PVA/WBPU = 7/3 and 5/5 electrodes maintained conductivity up to 80% strain, but with markedly different electromechanical responses. The 7/3 electrode exhibited a steep increase in resistance, reaching more than a 100-fold increase at 60% strain. In contrast, the 5/5 electrode showed significantly enhanced strain tolerance, with only a 10-fold increase in resistance at 60% strain and a 15-fold increase at 80% strain. These results indicate that the stretchability of nanomesh electrodes improves with WBPU incorporation, with the optimal performance achieved at a ratio of 5/5.

In practical applications, skin impedance is known to exceed double its baseline value and become unstable when electrode resistance rises above ~1 kΩ. Since the initial resistance of the nanomesh electrodes was in the range of 10–100 Ω, electrodes with $R/R_0 > 100$ can be considered unsuitable for practical use. Additionally, considering that the maximum elongation of human skin is approximately 66%[22], electrodes intended for skin applications should maintain $R/R_0 < 100$ at strains up to ~70%. Based on this criterion, the PVA/WBPU = 5/5 nanomesh electrode is the most stable and practical among those tested.

The electromechanical durability of the PVA-only and PVA/WBPU = 5/5 electrodes was further compared under repeated stretching. Figure 3e shows resistance changes during 1000 stretch–release cycles at 20% strain. The PVA-only electrode failed rapidly, with resistance increasing tenfold within 30 cycles and rupture occurring at 160 cycles. By contrast, the 5/5 electrode exhibited only a gradual increase in resistance, retaining conductivity after 1000 cycles (110 Ω at 0% strain and 320 Ω at 20% strain). These results confirm that blending PVA with WBPU markedly enhances stretchability and durability, with the 5/5 composition providing the best electromechanical performance.

Skin impedance/resistance measurement using PVA/WBPU blend nanomesh electrodes

To evaluate whether the PVA/WBPU blend nanomesh electrodes can reliably capture changes in skin impedance, a film cover experiment was performed. As shown in Fig. 4a, a pair of PVA-only electrodes and a pair of PVA/WBPU = 5/5 electrodes were attached to the subject's right forearm, approximately 5 cm from the wrist. Skin impedance at 1 kHz was continuously measured. Ten minutes after the start of the measurement, the measurement area was covered with a non-breathable plastic film for 1 min, followed by 1 min of uncovering. This cycle was repeated three times.

The results, presented in Fig. 4b, show that both the PVA-only and the PVA/WBPU = 5/5 electrodes detected reproducible fluctuations in impedance corresponding to the film covering and uncovering. These results are consistent with earlier reports using PVA-only nanomesh electrodes, which highlighted the critical importance of electrode breathability for skin resistance monitoring[10]. The present findings confirm that, in addition to improved water and strain stability, the PVA/WBPU blend nanomesh electrodes maintain the necessary breathability to enable reliable, real-time monitoring of skin impedance.

Long-term on-skin stability of PVA/WBPU blend nanomesh electrodes

To evaluate the long-term electrical stability of the nanomesh electrodes on skin, pairs of PVA-only and PVA/WBPU = 5/5 electrodes were attached to the forearm (Fig. 5a) and palm (Fig. 5c). The resistance of each electrode was monitored over several hours to compare the performance of conventional PVA-only nanomesh electrodes with that of the blend electrodes. Note that the forearm and palm measurements were conducted on different subjects to account for variations in skin properties between these regions.

On the forearm, PVA-only electrodes initially exhibited resistances around 100 Ω. Some samples maintained relatively stable values over several hours, but others showed a rapid increase, exceeding 1 kΩ within 6 h, and in certain cases complete disconnection occurred (Fig. 5b). In contrast, all of the PVA/WBPU = 5/5 electrodes showed consistently low and stable resistance values, remaining within 10–30 Ω throughout the same period. Quantitatively, only 2 out of 6 PVA-only electrodes (33%) retained resistances below 1 kΩ after 6 h, whereas all 6 of the PVA/WBPU = 5/5 electrodes (100%) remained below this threshold (Fig. 5e). These findings indicate that the blend electrodes provide reproducible electrical stability, unlike the variable performance of PVA-only electrodes.

A similar trend was observed on the palm, where sweat and motion impose more severe conditions. Among the PVA-only electrodes, some retained stable resistance, but many exhibited large increases within 1–2 h, frequently surpassing 1000 Ω or failing entirely with slight movement (Fig. 5d). Quantitatively, only 3 out of 8 PVA-only electrodes (38%) maintained resistances below 1 kΩ after 4 h, whereas all 8 of the PVA/WBPU = 5/5 electrodes (100%) remained below 50 Ω throughout the same period. This variability in the PVA-only samples resulted in poor reproducibility of skin impedance measurements, while the blend electrodes enabled reliable measurements even under high-sweat conditions.

The observed differences are attributed to the structural composition of the electrodes. In PVA-only electrodes, dissolution of PVA in sweat leaves only the Au nanomesh, which is prone to fracture when pressed into skin grooves, resulting in unstable resistance or disconnection. In contrast, in PVA/WBPU = 5/5 electrodes, tubular PU fibers remain after partial dissolution of PVA, reinforcing the structure and preventing Au rupture.

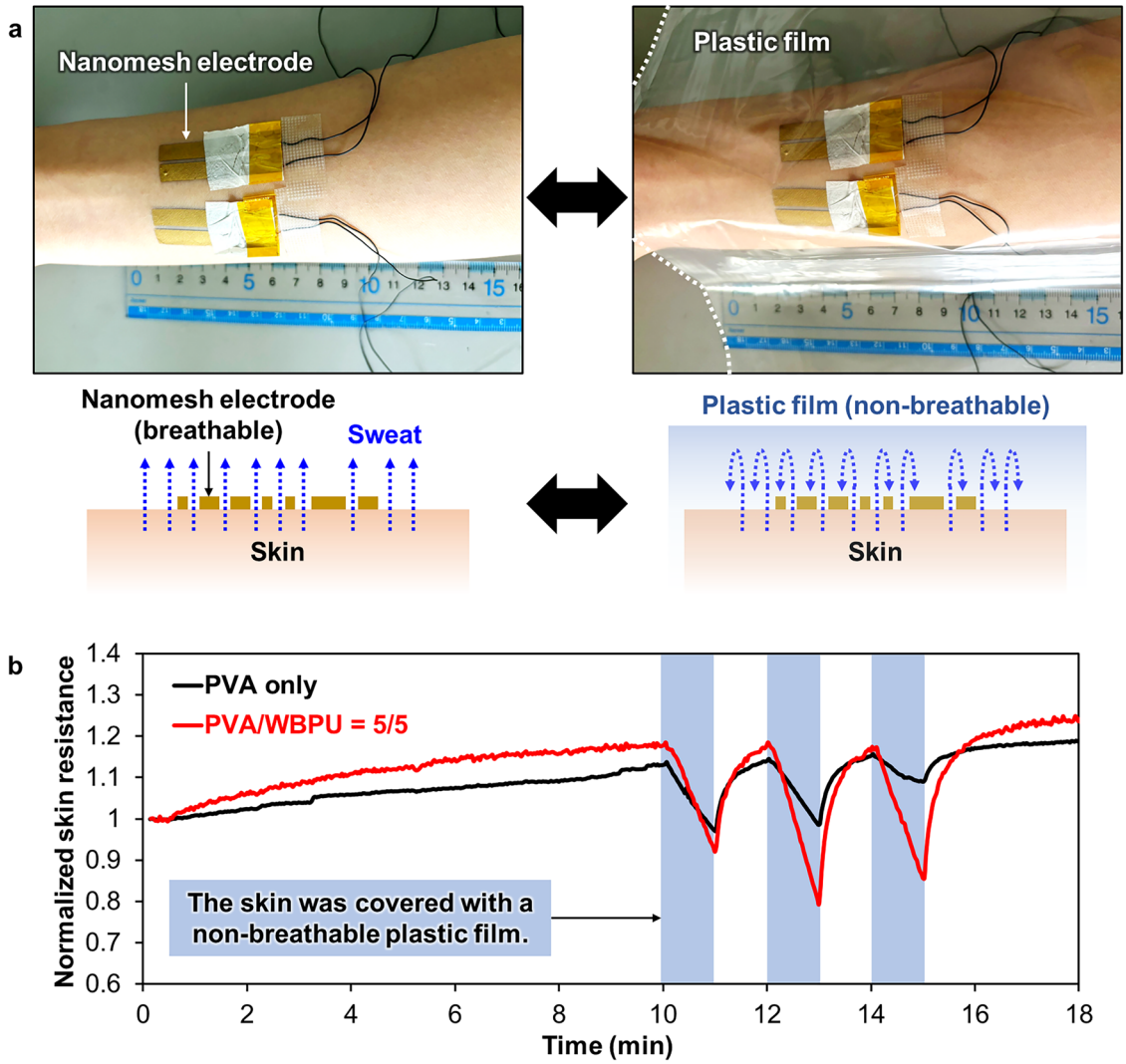

Fig. 4 | Skin impedance measurement using nanomesh electrodes. a Photographs and schematic illustrations of the experimental setup for skin impedance measurement. PVA/WBPU = 5/5 and PVA-only nanomesh electrodes were attached to the forearm skin. During the measurement, the electrodes were covered with a non-breathable plastic film to suppress natural evaporation and to accentuate the effect of sweat accumulation beneath the electrodes. **b** Skin impedance recorded at a measurement frequency of 1 kHz. Both PVA/WBPU = 5/5 and PVA-only nanomesh electrodes clearly captured the decrease in skin resistance when sweat evaporation was blocked by the non-breathable plastic film, demonstrating their ability to detect sweat-induced impedance changes.

Consequently, the PVA/WBPU blend architecture ensures both mechanical robustness and electrical reliability under dynamic, high-humidity conditions, leading to reproducible performance across different skin sites and users. These results clarify that the incorporation of WBPU into the PVA nanomesh effectively enhances the electrode's mechanical robustness and electrical stability under wet and deformable skin conditions, enabling reliable long-term skin impedance measurement.

This study demonstrated that blending PVA with WBPU yielded nanomesh electrodes that combine water resistance, stretchability, and breathability. Structural analyses revealed a phase-separated morphology in which PVA domains dissolve to provide adhesion, while WBPU fibers remain to reinforce the mesh network. By optimizing the blend ratio to PVA/WBPU = 5/5, the electrodes maintained stable electrical resistance and mechanical integrity for at least 4 h even on the palm, where sweating and motion impose severe stress. These results clarify that controlling the polymer composition enables stable performance of breathable nanomesh electrodes under dynamic and humid skin conditions. In principle, higher WBPU fractions may further improve mechanical robustness; however, in this study WBPU was used as a commercially supplied aqueous dispersion, and reducing the water content raised concerns regarding phase separation or material alteration. Therefore, optimization was performed within the practical constraints of the selected materials, yielding PVA/WBPU = 5/5 as the optimal composition.

While this work establishes the fundamental advantage of polymer blending for improving the durability of nanomesh electrodes, several challenges remain for future translation. In particular, achieving reliable electrical interconnection between the nanomesh and external systems, integrating stretchable wiring, and combining the electrodes with wireless modules will be important for realizing practical long-term monitoring devices. Future studies should also extend evaluation toward chronic applications and assess the clinical relevance of continuous skin impedance monitoring. Overall, this study demonstrates the scientific significance of optimizing polymer blend ratios as a materials design strategy to ensure the electrical and mechanical stability of breathable nanomesh electrodes.

Methods

Materials

Polyvinyl alcohol (EG-22P & EG-48P) were purchased from the Nippon Synthetic Chemical Industry Co., Ltd., Tokyo. Waterborne polyurethane (ETERNACOLL® UW-1005E) was supplied from UBE Corporation,

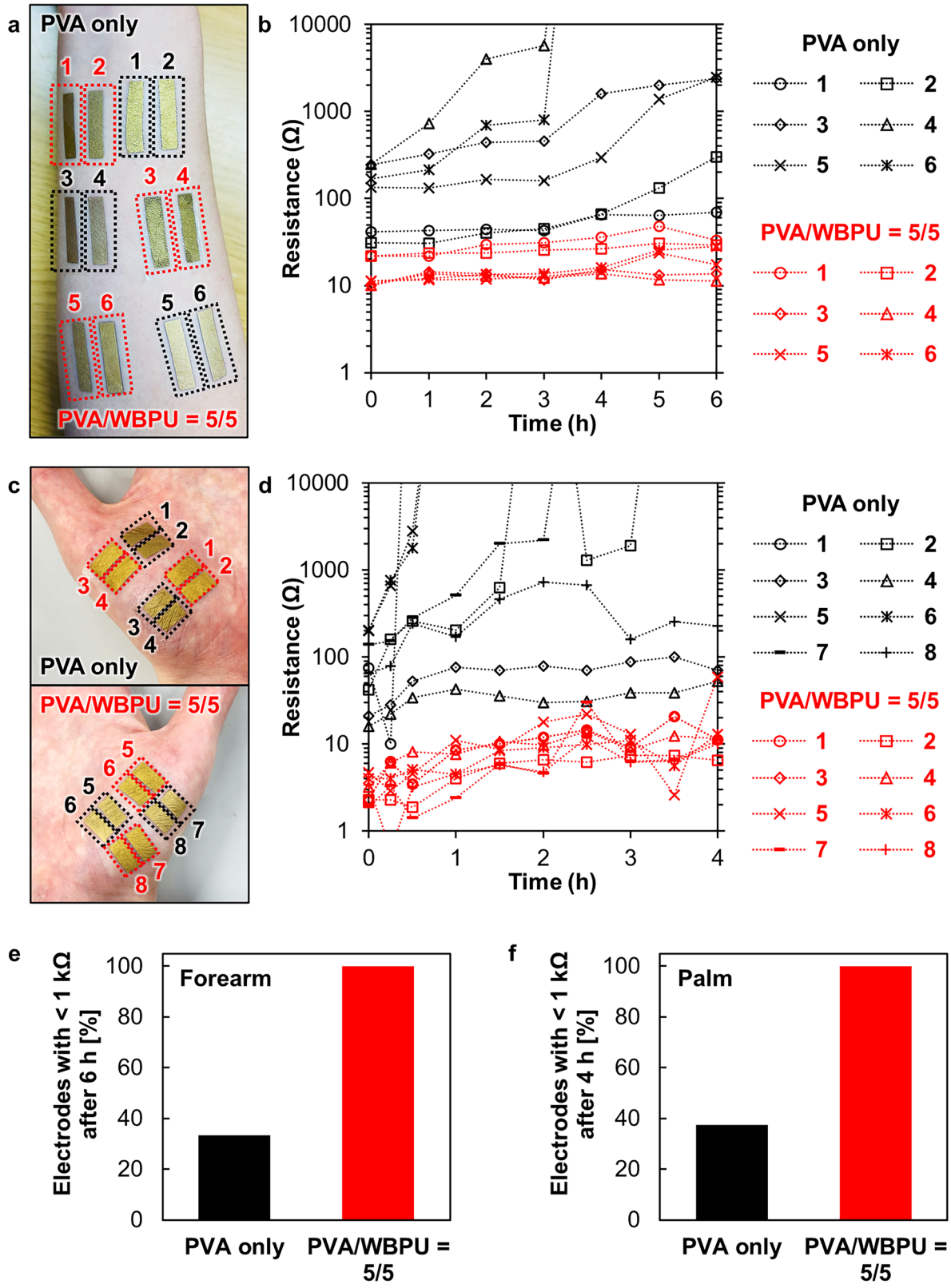

Tokyo, as an aqueous dispersion and was used as received without further dilution or modification. Artificial skin sheets (BIO SKIN PLATE 100 μm) for water stability test were purchased from Beaulax, Saitama. Artificial skin sheets (2-mm-thick, 7-8319-01) for the stretchability test were purchased from AS ONE Corporation, Osaka.

Preparation of solutions

First, 2.0 g of PVA (EG-22P) powder and 1.0 g of PVA (EG-48P) powder were added to 27 g of pure water and stirred at 70 °C for 2 h, followed by overnight stirring at room temperature to obtain a 10 wt% PVA solution for conventional nanomesh electrodes. A 15 wt% PVA solution for blend

Fig. 5 | Long-term stability of PVA/WBPU blend nanomesh electrodes on skin. **a** Photographs of PVA/WBPU = 5/5 and PVA-only nanomesh electrodes attached to the forearm for long-term evaluation. **b** Relative resistance of 12 electrodes on the forearm over time. PVA/WBPU = 5/5 electrodes exhibited stable resistance values with minimal drift, whereas PVA-only electrodes showed large fluctuations and eventual failure due to loss of adhesion. **c** Photographs of PVA/WBPU = 5/5 and PVA-only nanomesh electrodes attached to the palm, a region subject to sweating and frequent deformation. **d** Relative resistance of 16 electrodes on the palm. The PVA/WBPU = 5/5 electrodes maintained stable conductivity, while PVA-only electrodes displayed unstable signals and rapid degradation. **e** Quantitative comparison of resistance stability on the forearm after 6 h. Only 2 out of 6 PVA-only electrodes (33%) maintained resistances below 1 kΩ, whereas all 6 of the PVA/WBPU = 5/5 electrodes (100%) remained within this range, confirming the reproducible electrical stability of the blend electrodes. **f** Quantitative comparison of resistance stability on the palm after 4 h. Only 3 out of 8 PVA-only electrodes (38%) maintained resistances below 1 kΩ, while all 8 of the PVA/WBPU = 5/5 electrodes (100%) remained below 50 Ω, demonstrating stable performance even under high-sweat and motion conditions.

nanomesh electrodes was prepared in the same manner by adjusting the amount of pure water.

A commercially supplied 30 wt% waterborne polyurethane (WBPU) aqueous dispersion was used as received without further dilution. The 15 wt % PVA solution and the 30 wt% WBPU dispersion were mixed at weight ratios of 18:1, 14:3, 2:1, 6:7, and 2:9. Each mixture was stirred for 1 h at room temperature to obtain PVA/WBPU solutions with polymer weight ratios of 9/1, 7/3, 5/5, 3/7, and 1/9, respectively.

Fabrication of nanomesh electrodes

Nanomesh electrodes were fabricated largely in accordance with the fabrication method reported in previous study[10,18]. First, six kinds of nanofibers were prepared from 10 wt% PVA and 5 kinds of PVA/WBPU blend solution by electrospinning method. Electrospinning machine (MECC, NANON-03) was used and applied voltage, needle-collector distance, feed rate, and solution volume were set at 25 kV, 12.5 cm, 0.6 mL/h, and 1.2 mL, respectively. Then nanofibers were heatpressed to enhance physical durability and conductivity as electrode[23]. PVA nanofiber sheets were heatpressed at the condition of 180 °C, 50 kPa, 1 min, same as the previous study. PVA/WBPU nanofiber sheets were heatpressed at the condition of 150 °C, 50 kPa, 1 min. Finally, 100-nm-thick of gold was deposited on each nanofiber sheets by thermal evaporation method (ULVAC, EX-200). Masks for patterning of gold were prepared by cutting 125-μm-thick polyimide films with green laser (Keyence, MD-T1000 Series).

Measurement of contact angle

Contact angle measurements were performed using the following procedure with a measuring instrument (Asumi Giken Co., Ltd., Contact Angle Tester B100). Each nanomesh electrode was peeled off from the cooking sheet and placed on a glass plate with the gold side up. Since the electrode is very thin, it was temporarily fixed with ethanol, and water was sprayed 2–3 times from a distance of 20 cm with a mist sprayer. After waiting for the surface to dry, it was set on the stand of the measuring instrument. Water was sucked into a syringe and droplets were created using a needle (30 G). The droplet size was adjusted to 1.00 ± 0.05 μL and the contact angle was measured for 20 s after adhesion to the interface.

Water-stability test

First, an artificial skin sheet was attached to an acrylic plate, and an I-shaped nanomesh electrode was attached on top of it. Conductors were connected to both ends of the electrode with Kapton tape and connected to a multimeter. The acrylic plate prepared in this way was stood on a container so that it was inclined at an angle of approximately 19°, and a hose was fixed over the acrylic plate so that it was perpendicular to the electrode. One minute after the start of electrode resistance measurement with the multimeter, water was flowed at approximately 1 MPa using a running water pump (Tsukasa Electric Works, Ltd., portable tube pump PP-DP1-200) The cross-section of the tube used was a circle with a diameter of 4 mm.

Tensile test

To evaluate the stretchability when the electrode was attached to the skin rather than the stretchability of the electrode itself, the tensile test was conducted by attaching the nanomesh electrode to an artificial skin sheet and applying strain to the sheet using a linear translation stage (Thorlabs, LTS150C). A 10 cm × 10 cm artificial skin sheet was cut into 15 rectangular pieces of 2 cm × 3.3 cm. A nanomesh electrode (0.6 cm × 2.4 cm) was attached to the center of each rectangle using water. The initial gap of the translation stage was set to 2.4 cm, and both ends of the artificial skin sheet were fixed using VHB™ tape (3 M) and Kapton tape. To measure the electrode resistance, liquid metal (galinstan) was used to connect copper wires to both ends of the electrode, which were then connected to a multimeter. Using this experimental setup, two types of experiments were conducted. In the first experiment, the stage was stretched by 10%, held for one minute, and the electrode resistance was measured repeatedly until the extension reached 80%. In the second experiment, the stage was alternately stretched by 20% and returned to 0%.

Measurement of skin impedance with an LCR meter

A pair of nanomesh electrodes was delaminated from a cooking sheet and placed on the forearm with the Au-coated side facing the skin. A small amount of water was sprayed to induce adhesion of the electrodes to the skin by taking advantage of the water solubility of PVA. An Au–PU nanomesh connector, fabricated in the same manner as described in a previous study[24], was then attached to the electrodes to establish electrical contact with the probes of an LCR meter (Agilent, E4980A). Skin impedance was measured at a frequency of 1 kHz.

Data availability

Data is provided within the manuscript or supplementary information files.

Received: 6 November 2025; Accepted: 26 January 2026;
Published online: 03 February 2026

References

1. Abe, T. Water and the skin. *Jpn. Oil Chem. Soc.* **34**, 413–419 (1985).
2. Vaughn, A. R., Clark, A. K., Sivamani, R. K. & Shi, V. Y. Natural oils for skin-barrier repair: ancient compounds now backed by modern science. *Am. J. Clin. Dermatol.* **19**, 103–117 (2018).
3. Kalia, Y. N., Nonato, L. B., Lund, C. H. & Guy, R. H. Development of skin barrier function in premature infants. *J. Investig. Dermatol.* **111**, 320–326 (1998).
4. Sharma, M., Kacker, S. & Sharma, M. A brief introduction and review on galvanic skin response. *Int. J. Med. Res. Prof.* **2**, 13–17 (2016).
5. Shi, Y., Ruiz, N., Taib, R., Choi, E. H. C. & Chen, F. Galvanic skin response (GSR) as an index of cognitive load. in *CHI EA '07: Extended Abstracts on Human Factors in Computing Systems* 2651–2656 (Assoc. Comput. Mach., 2007).
6. Alexander, H., Brown, S., Danby, S. & Flohr, C. Research techniques made simple: transepidermal water loss measurement as a research tool. *J. Investig. Dermatol.* **138**, 2295–2300.e1 (2018).
7. Asahina, M., Poudel, A. & Hirano, S. Sweating on the palm and sole: physiological and clinical relevance. *Clin. Auton. Res.* **25**, 153–159 (2015).
8. Asahina, M., Suzuki, A., Mori, M., Kanesaka, T. & Hattori, T. Emotional sweating response in a patient with bilateral amygdala damage. *Int. J. Psychophysiol.* **47**, 87–93 (2003).
9. Agache, P. G., Monneur, C., Leveque, J. L. & De Rigal, J. Mechanical properties and Young's modulus of human skin in vivo. *Arch. Dermatol. Res.* **269**, 221–232 (1980).

10. Miyamoto, A. et al. Highly precise, continuous, long-term monitoring of skin electrical resistance by nanomesh electrodes. *Adv. Healthc. Mater.* **11**, e2200763 (2022).
11. Yao, S. et al. A wearable hydration sensor with conformal nanowire electrodes. *Adv. Healthc. Mater.* **6**, 1601159 (2017).
12. Park, S. H., Park, J., Park, H. N., Park, H. M. & Song, J. Y. Flexible galvanic skin response sensor based on vertically aligned silver nanowires. *Sens. Actuators B Chem.* **273**, 804–808 (2018).
13. Luo, J. et al. On-skin paintable water-resistant biohydrogel for wearable bioelectronics. *Adv. Funct. Mater.* **34**, 2401234 (2024).
14. Han, I. K. et al. Electroconductive, adhesive, non-swelling, and viscoelastic hydrogels for bioelectronics. *Adv. Mater.* **35**, 2208981 (2023).
15. Jang, H. et al. Graphene e-tattoos for unobstructive ambulatory electrodermal activity sensing on the palm enabled by heterogeneous serpentine ribbons. *Nat. Commun.* **13**, 6604 (2022).
16. McAdams, E. T., Jossinet, J., Lackermeier, A. & Risacher, F. Factors affecting electrode-gel-skin interface impedance in electrical impedance tomography. *Med. Biol. Eng. Comput.* **34**, 397–408 (1996).
17. Li, G., Wang, S. & Duan, Y. Y. Towards gel-free electrodes: a systematic study of electrode-skin impedance. *Sens. Actuators B Chem.* **241**, 1244–1255 (2017).
18. Miyamoto, A. et al. Inflammation-free, gas-permeable, lightweight, stretchable on-skin electronics with nanomeshes. *Nat. Nanotechnol.* **12**, 907–913 (2017).
19. Haider, S. et al. Highly aligned narrow diameter chitosan electrospun nanofibers. *J. Polym. Res.* **20**, 105 (2013).
20. Mohammad Ali Zadeh, M., Keyanpour-Rad, M. & Ebadzadeh, T. Effect of viscosity of polyvinyl alcohol solution on morphology of the electrospun mullite nanofibres. *Ceram. Int.* **40**, 5461–5466 (2014).
21. Kwok, D. Y. & Neumann, A. W. Contact angle measurement and contact angle interpretation. *Adv. Colloid Interface Sci.* **81**, 167–249 (1999).
22. Harada, T., Tsuchida, K., Fusaka, K. & Iriya, M. Body skin strain and stretch properties of fabrics. *J. Text. Mach. Soc. Jpn.* **36**, P275–P279 (1983).
23. Okutani, C., Yokota, T. & Someya, T. Interconnected heat-press-treated gold nanomesh conductors for wearable sensors. *ACS Appl. Nano Mater.* **3**, 1848–1854 (2020).
24. Papanastasiou, D. T. et al. A novel thickness-gradient electrospun nanomesh for interface-free e-skin applications. *Mater. Horiz.* **12**, 4676–4684 (2025).

Acknowledgements

The authors declare no additional acknowledgements. This research was supported by AMED under Grant Number JP223fa627001 and the JST, CREST Grant Number JPMJCR21P2.

Author contributions

M.M., Y.E., X.L., and D.I. conducted the experiments. M.M. and K.Y. wrote the manuscript and prepared the figures. D.H., S.L., T.Y., K.Y., and T.S. reviewed and revised the manuscript. S.L., T.Y., K.Y., and T.S. supervised the project. All authors discussed the results and approved the final manuscript.

Competing interests

Author Takao Someya is Editorial Board Members of npj Flexible Electronics. Takao Someya was not involved in the journal's review of, or decisions related to, this manuscript. The other Authors declare no Competing Financial or Non-Financial Interests.

Additional information

Supplementary information The online version contains supplementary material available at https://doi.org/10.1038/s41528-026-00542-8.

Correspondence and requests for materials should be addressed to Takao Someya.